Preparations, Structures, Electronic Structures, and Magnetic Properties of Face-Sharing Bioctahedral Niobium(III) and Tantalum(III) Compounds

F. Albert Cotton,*,† Xuejun Feng,† Philipp Gütlich,‡ Thomas Kohlhaas,‡ Jian Lu,† and Maoyu Shang†

Department of Chemistry and Laboratory for Molecular Structure and Bonding, Texas A&M University, College Station, Texas 77843, and Institute for Inorganic Chemistry and Analytical Chemistry, Johannes Gutenberg-Universität Mainz, Staudinger Weg 9, D-6500 Mainz, Germany

Received December 22, 1993®

Four face-sharing bioctahedral anions containing niobium and tantalum have been obtained in crystalline compounds and structurally characterized. The following compounds and their crystal structures are reported. $(Et_4N)_2[Nb_2Cl_8(THT)]$: *Pcca*, $a = 29.602(5)$ Å, $b = 16.057(3)$ Å, $c = 14.338(3)$ Å, $V = 6815(2)$ Å^3, $Z = 8$; the THT (tetrahydrothiophene) sulfur atom occupies a bridging position and Nb–Nb = 2.707(2) Å. $(Et_4N)_3[Nb_2Cl_9]\cdot 5CH_2Cl_2$: *C*2, $a = 18.338(3)$ Å, $b = 14.126(3)$ Å, $c = 11.747(2)$ Å, $\beta = 114.70(1)°$, $V = 2765(1)$ Å^3, $Z = 2$; the anion has an Nb–Nb distance of 2.7413(3) Å. $(Pr_4N)_3[Nb_2Cl_9]\cdot 6CH_2Cl_2$: *Iba*2, $a = 17.235(4)$ Å, $b = 45.588(7)$ Å, $c = 18.604(4)$ Å, $V = 14{,}617(5)$ Å^3, $Z = 8$; Nb–Nb = 2.691(2) Å. $(Et_4N)_2[Ta_2Cl_8(THT)]$: *Pcca*, $a = 29.577(4)$ Å, $b = 16.046(3)$ Å, $c = 14.332(1)$ Å, $V = 6802(2)$ Å^3, $Z = 8$; this compound, isomorphous with its Nb analog, has Ta–Ta = 2.6875(8) Å. Variable-temperature magnetic susceptibilities are reported for $(Et_4N)_2[Nb_2Cl_8(THT)]$ and a previously reported compound, $(Bu_4N)[Nb_2Cl_7(PEt_3)_2]$. In both cases, the susceptibilities were found to be temperature independent over a wide temperature range. Electronic structures of the model species $[Nb_2Cl_9]^{3-}$, $[Nb_2Cl_7(PH_3)_2]^-$, and $[Nb_2Cl_8(\mu\text{-}SH_2)]^{2-}$ were studied by employing quantum chemical calculations in which both the SCF–Xα–SW molecular orbital method and the ab initio configuration interaction method were employed. The results of the calculations indicate that the metal–metal interaction in each type of face-sharing compound can be formally described by a double bond although the π component is relatively weak. On the basis of the calculated electronic structures, a satisfactory explanation can be obtained for the observed temperature-independent paramagnetism of the compounds.

Introduction

Dinuclear niobium(III) complexes with face-sharing bioctahedral structures have been known for many years, but relatively few have been well characterized. The first to be reported were the $[Nb_2X_9]^{3-}$ species,[1] of which the $[Nb_2Cl_9]^{3-}$ ion as its cesium salt will be of interest here. Next, there were reports of structurally characterized compounds containing a bridging SR_2 ligand (along with two μ-Cl or μ-Br ligands) but also having two neutral terminal ligands in positions trans to the μ-SR_2 ligands, namely, $Nb_2Cl_6(\mu\text{-}SMe_2)(C_4H_8O)_2$,[2] $Nb_2Cl_6(\mu\text{-}C_4H_8S)(C_4H_8O)_2$,[3] $Nb_2Cl_6(\mu\text{-}C_4H_8S)(PEt_3)_2$,[3] and $Nb_2Br_6(\mu\text{-}C_4H_8S)(C_4H_8S)_2$.[4] Compounds containing a $[Nb_2Cl_8(\mu\text{-}C_4H_8S)]^{2-}$ ion have been mentioned,[5] but none has heretofore been structurally characterized. It is only recently that compounds of the $[Nb_2Cl_7(PR_3)_2]^-$ ions (R = Me, Et) were prepared and structurally characterized.[6] It may be noted that there are tantalum analogs for some but not all of these niobium compounds.[7]

Since all of these dinuclear species contain two M(III) components in relatively close proximity, each with a d^2 configuration, there can be no doubt that electronic interactions occur between them. However, the nature of these interactions has been sketchily defined by the limited structural data and the fragmentary magnetic data, not to mention the complete lack of any reasonably rigorous theoretical work. The study reported here has the threefold purpose of beginning to fill these gaps, namely, (1) to provide structural data on two important species, $[Nb_2Cl_8(THT)]^{2-}$ and $[Nb_2Cl_9]^{3-}$, for which few or none were heretofore available, (2) to obtain magnetic data for several compounds over a wide temperature range, and (3) to present the results of thorough and rigorous molecular orbital calculations.

In the following pages, we will first report the preparation and structural characterization by X-ray crystallography of four compounds that contain $[Nb_2Cl_9]^{3-}$, $[Nb_2Cl_8(THT)]^{2-}$, and $[Ta_2Cl_8(THT)]^{2-}$ ions. The results of theoretical computations on the electronic structures of several of the face-sharing compounds will also be given. The calculations have been performed by both the SCF–Xα–SW method and the ab initio configuration interaction (CI) method on model niobium compounds. Finally, we shall present a complete study of the magnetic properties of the niobium compounds $(Bu_4N)[Nb_2Cl_7(PR_3)_2]$ and $(Et_4N)_2[Nb_2Cl_8(THT)]$. Studies of the magnetic properties and electronic structure of the $[Nb_2Cl_9]^{3-}$ ion will be described in a later paper.

Experimental Section

General Procedures. All synthetic work and sample handling were performed by employing standard Schlenk techniques and a drybox under an atmosphere of argon or dinitrogen. Solvents benzene and hexane were refluxed over Na–K alloy/benzophenone, dichloromethane was refluxed over phosphorus pentoxide, and absolute ethanol was refluxed over Mg turnings for at least 8 h and distilled freshly prior to use. $Et_4NCl\cdot XH_2O$ was purchased from Sigma Chemical Co. and dried by consecutive azeotropic distillation in EtOH and benzene. Anhydrous

† Texas A&M University.
‡ Johannes Gutenberg-Universität.
* Abstract published in *Advance ACS Abstracts*, June 1, 1994.

(1) Broll, A.; von Schnering, H. G.; Schafer, H. *J. Less-Common Met.* **1970**, *22*, 243.
(2) Cotton, F. A.; Duraj, S. A.; Roth, W. J. *Acta Crystallogr.* **1985**, *C41*, 878.
(3) Babaian-Kibala, E.; Cotton, F. A.; Shang, M. *Acta Crystallogr.* **1991**, *C47*, 1617.
(4) Templeton, J. L.; Dorman, W. C.; Clardy, J. C.; McCarley, R. E. *Inorg. Chem.* **1978**, *17*, 1263.
(5) Maas, E. T., Jr.; McCarley, R. E. *Inorg. Chem.* **1973**, *12*, 1096.
(6) Cotton, F. A.; Shang, M. *Inorg. Chem.* **1993**, *32*, 969.
(7) (a) Cotton, F. A.; Najjar, R. C. *Inorg. Chem.* **1981**, *20*, 2716. (b) Cotton, F. A.; Falvello, L. R.; Najjar, R. C. *Inorg. Chim. Acta* **1982**, *63*, 107. (c) Gilletti, P. F.; Young, V. G.; Brown, T. M. *Inorg. Chem.* **1989**, *28*, 4034.

0020-1669/94/1333-3055$04.50/0

Table 1. Crystal Data for $(Et_4N)_3[Nb_2Cl_9]\cdot 5CH_2Cl_2$, $(Pr_4N)_3[Nb_2Cl_9]\cdot 6CH_2Cl_2$, $(Et_4N)_2[Ta_2Cl_8(THT)]$, and $(Et_4N)_2[Nb_2Cl_8(THT)]$

formula	$Nb_2Cl_{19}N_3C_{29}H_{70}$	$Nb_2Cl_{21}N_3C_{42}H_{96}$	$Ta_2Cl_8SN_2C_{20}H_{48}$	$Nb_2Cl_8SN_2C_{20}H_{48}$
fw	1320.32	1573.58	994.20	818.12
space group	*C*2	*Iba*2	*Pcca*	*Pcca*
a, Å	18.338(3)	17.235(4)	29.577(4)	29.602(5)
b, Å	14.126(3)	45.588(7)	16.046(3)	16.057(3)
c, Å	11.747(2)	18.604(4)	14.332(1)	14.338(1)
α, deg	90.0	90.0	90.0	90.0
β, deg	114.70(1)	90.0	90.0	90.0
γ, deg	90.0	90.0	90.0	90.0
V, Å^3	2764.6(9)	14617(5)	6802(2)	6815(2)
Z	2	8	8	8
d_{calc}, g/cm^3	1.586	1.430	1.942	1.595
μ(Mo Kα), cm^{-1}	13.502	11.051	182.805	13.510
radiation monochromated in incident beam: λ(Mo Kα), Å	0.710 73	0.710 73	1.541 84	0.710 73
temp, °C	−60	−60	20	20
transm factors: max, min	0.9998, 0.8867	0.9983, 0.8333	1.0000, 0.4389	0.9993, 0.8313
R_1[a]	0.024	0.065	0.051	0.051
R_2[b]	0.034	0.079	0.065	0.065

[a] $R_1 = \sum||F_o| - |F_c||/\sum|F_o|$. [b] $R_2 = [\sum w(|F_o| - |F_c|)^2/\sum w|F_o|^2]^{1/2}$; $w = 1/\sigma^2(|F_o|)$.

Pr_4NCl was from Chemlog Co. and was used as received. $Nb_2Cl_6L_3$ (L = THT, Me_2S)[8] and $Ta_2Cl_6L_3$ (L = Me_2S, THT)[9] were prepared by the literature methods. Single-crystal X-ray diffraction work was performed on either a CAD4, an AFC5R, or a P3-equivalent diffractometer at 20 or −60 °C.

Preparation of $(Et_4N)_2[Nb_2Cl_8(THT)]$. A modification of the literature method[5] was necessary to obtain large crystals. A benzene solution (25 mL) of $Nb_2Cl_6(THT)_3$ (0.332 g, 0.5 mmol) was layered on a CH_2Cl_2 solution (15 mL) of Et_4NCl (0.33 g, 2 mmol) in a Schlenk tube. Purple platelike crystals grew on the walls above the solvent interface during about 5 days of solvent diffusion. A small amount of brown fluffy precipitate which deposited on the bottom of the tube was separated from the crystals by stirring the mixture in the mother liquor or a solvent mixture of benzene and dichloromethane (2:1 in volume) and decanting the liquid phase after the crystals had settled down. Yields were 70–80%. With longer diffusion times, generally after 10 days, we observed the formation of gray-blue platelike crystals on the bottom or on the walls of the lower part of the tube. These were later characterized as $(Et_4N)_3[Nb_2Cl_9]\cdot XCH_2Cl_2$.

Preparation of $(Et_4N)_2[Ta_2Cl_8(THT)]$. A slightly different stoichiometry was used to prepare the tantalum analogue. The upper layer was a benzene solution (15 mL) of $Ta_2Cl_6(THT)_3$ (0.21 g, 0.25 mmol), and the lower layer was a dichloromethane solution (15 mL) of Et_4NCl (0.17 g, 1 mmol). Brown, block-shaped crystals were formed in a week along with a small quantity of brown-blue precipitate. Yields fell in the range 70–90%. No further reaction, such as the formation of a nonachloride, was observed even after 2 months of standing. When $Ta_2Cl_6(Me_2S)_3$ was used instead of $Ta_2Cl_6(THT)_3$ and Pr_4NCl was used instead of Et_4NCl, sometimes after 1 or 2 months of standing, along with the major product (brown crystals, presumably containing $[Ta_2Cl_8(Me_2S)]^-$), a small amount of colorless block-shaped crystals were formed, which were characterized later as $(Pr_4N)_2[Ta_2OCl_{10}]$.[10]

Preparation of $(Et_4N)_3[Nb_2Cl_9]\cdot XCH_2Cl_2$. Method 1. $Nb_2Cl_6(THT)_3$ (0.166 g, 0.25 mmol) and Et_4NCl (0.24 g, 1.5 mmol) were dissolved in CH_2Cl_2 (20 mL). The solution was left undisturbed for 3 weeks. When the solution was kept at room temperature (26 °C), hexagonal platelike blue-gray crystals were formed, while, at 0 °C in a refrigerator, gray slab-shaped crystals were formed. X-ray structure analysis showed later that the quantities of interstitial solvent CH_2Cl_2 were different in the two cases. However, the yields were approximately the same: ca. 75%.

Method 2. $Nb_2Cl_6(Me_2S)_3$ (0.146 g, 0.25 mmol) and Et_4NCl (0.25 g, 1.5 mmol) were dissolved in CH_2Cl_2 (30 mL), and the solution was kept at 0 °C for a week. Long gray-blue platelike crystals (sometimes 1 cm in length) were formed. A typical yield was 92%.

Preparation of $(Pr_4N)_3[Nb_2Cl_9]\cdot 6CH_2Cl_2$. $Nb_2Cl_6(Me_2S)_3$ (0.073 g, 0.13 mmol) and Pr_4NCl (0.167 g, 0.75 mmol) were dissolved in CH_2Cl_2 (10 mL), and the solution was kept at 26 °C for a week. Light gray-blue, rectangular platelike crystals were formed. Yield: ca. 40%. When $Nb_2Cl_6(THT)_3$ was used instead of $Nb_2Cl_6(Me_2S)_3$, a similar yield was obtained, but the product belonged to a different crystal phase, as described below.

X-ray Crystallography for $(Et_4N)_3[Nb_2Cl_9]\cdot 5CH_2Cl_2$. Crystals which were grown at 0 °C were examined under a layer of mother liquor in a small dish that was kept in a fritted funnel and flushed constantly from the collection end of the funnel by a stream of argon. A suitable crystal was mounted on the top of a glass fiber by Apiezon T grease and transferred immediately to a goniometer head under a nitrogen flow at −60 °C. Unit cell parameters were refined by centering 25 reflections in the 2θ range 33–36°.[11] These parameters and the *C*-centered monoclinic crystal system were confirmed by axial photography. Three intensity standards, checked after every 2 h of data collection, showed a total of 5.5% decay during a total of 34.5 h of crystal exposure time, and an anisotropic decay correction was applied to the data set. Apart from the decay correction, corrections for Lorentz and polarization effects and for absorption (based on ψ scans of seven reflections with their χ Eulerian angles near 90°) were also applied. The Nb_2Cl_9 unit was revealed by the Patterson method[12] in the C2 space group, which was later confirmed to be the correct one by the successful solution and refinement of the entire structure. The remaining non-hydrogen atoms were found by a combination of least-squares refinements and difference Fourier syntheses. After all these atoms had been refined anisotropically, a difference Fourier synthesis revealed all the hydrogen atoms, which were then included in the structure factor calculation in the final full-matrix least-squares refinement. For 2505 unique reflections with $F_o^2 > 3\sigma(F_o^2)$ and 240 variables, the refinement converged with $R_1 = 0.024\,28$, $R_2 = 0.034\,41$, and a goodness-of-fit indicator of 1.213. The refinement of its enantiomorph resulted in marginally higher values, 0.024 29, 0.034 63, and 1.221, respectively. Although the second enantiomorph could not be completely ruled out, the first choice was retained. The dimensions of the $[Nb_2Cl_9]^-$ ion were not significantly different in the two cases, nor did the choice of chirality have any influence on the other structural parameters. No further effort was made to confirm the enantiomorph. Crystal data are listed in Table 1. Positional and equivalent isotropic thermal parameters of non-hydrogen atoms are listed in Table 2. Selected bond distances and angles are given in Table 3. The $[Nb_2Cl_9]^{3-}$ ion and its atom labels are shown in Figure 1a.

X-ray Crystallography for $(Et_4N)_3[Nb_2Cl_9]\cdot XCH_2Cl_2$. Crystals with a hexagonal platelike shape which were formed at 26 °C were handled in the same way as the above pentasolvate. The hexagonal Laue class 6/*mmm* and the cell parameters, $a = b = 10.235(2)$ Å, $c = 22.109(3)$ Å, and $V = 2005.8(7)$ Å^3, were verified by axial photography. Systematic absences and the averaging of equivalent reflections also attested to the Laue class and suggested as a possible space group $P6_3/mmc$. The Nb_2Cl_9 unit was found and refined without much difficulty, with the metal atoms situated on a 3-fold axis. This gave an *R* value of 0.12. However, the isotropic thermal parameters of these atoms were high (8 Å^2 for metal atoms and 12 Å^2 for chlorine atoms) and the tetraethylammonium

(8) Allen, A. D.; Naito, S. *Can. J. Chem.* **1976**, *54*, 2948.
(9) Templeton, J. L.; McCarley, R. E. *Inorg. Chem.* **1978**, *17*, 2293.
(10) Crystal data: space group $P\bar{1}$; $a = 9.956(2)$, $b = 10.953(2)$, $c = 11.079(2)$ Å; $\alpha = 74.16(1)$, $\beta = 63.88(2)$, $\gamma = 72.29(1)°$; $V = 1019.6(4)$ Å^3; $Z = 1$; 2558 observable intensity data ($F_o^2 > 3\sigma(F_o^2)$), 290 variables; $R_1 = 0.016$, $R_2 = 0.023$.
(11) Calculations were done on a Local Area VAX Cluster with the commercial package SDP/VAX, unless otherwise stated.
(12) Sheldrick, G. M. SHELXS-86: Program for X-ray Crystal Structure Determination. University of Göttingen, Germany, 1986.

Table 2. Positional and Equivalent Isotropic Thermal Parameters for $(Et_4N)_3[Nb_2Cl_9]\cdot 5CH_2Cl_2$

atom	x	y	z	B_{eq},[a] Å^2
Nb	0.56186(1)	0.500	0.11728(2)	1.712(5)
Cl(1)	0.500	0.35086(9)	0.000	2.51(3)
Cl(2)	0.42811(5)	0.57247(9)	0.07104(8)	2.91(2)
Cl(3)	0.62227(5)	0.64193(8)	0.23901(8)	3.04(2)
Cl(4)	0.55563(5)	0.42330(8)	0.30154(7)	2.67(2)
Cl(5)	0.69631(5)	0.43490(8)	0.16806(8)	2.97(2)
N(1)	0.500	0.6876(3)	0.500	2.23(9)
C(1)	0.4765(2)	0.7482(3)	0.3830(3)	2.91(8)
C(2)	0.4101(3)	0.8182(4)	0.3617(4)	4.4(1)
C(3)	0.5700(2)	0.6275(3)	0.5042(3)	2.74(8)
C(4)	0.6024(3)	0.5589(4)	0.6131(4)	4.0(1)
N(2)	0.1761(2)	0.7467(3)	0.8311(3)	2.58(7)
C(5)	0.1636(2)	0.8489(3)	0.8617(4)	3.16(9)
C(6)	0.2307(3)	0.9150(4)	0.8746(5)	4.4(1)
C(7)	0.2545(2)	0.7070(4)	0.9280(4)	3.07(8)
C(8)	0.2613(3)	0.7083(4)	1.0595(4)	4.5(1)
C(9)	0.1045(2)	0.6917(4)	0.8304(4)	3.7(1)
C(10)	0.1057(3)	0.5870(4)	0.8064(5)	5.1(1)
C(11)	0.1810(3)	0.7391(4)	0.7074(4)	3.27(9)
C(12)	0.1070(4)	0.7721(5)	0.5954(5)	5.1(1)
C(13)	0.500	0.8027(6)	0.000	4.9(2)
Cl(6)	0.4554(1)	0.8706(2)	0.0761(2)	7.10(4)
C(14)	0.6291(3)	0.2070(4)	0.2401(5)	4.4(1)
Cl(7)	0.6017(1)	0.1022(1)	0.1568(1)	6.77(4)
Cl(8)	0.71998(8)	0.2003(1)	0.3723(2)	6.99(4)
C(15)	0.8011(4)	0.4716(4)	0.5070(5)	5.2(1)
Cl(9)	0.82571(9)	0.3760(1)	0.6125(1)	6.40(4)
Cl(10)	0.8904(1)	0.5313(1)	0.5241(1)	6.10(3)

[a] Anisotropically refined atoms are given in the form of the equivalent isotropic displacement parameter defined as $(4/3)[a^2\beta_{11} + b^2\beta_{22} + c^2\beta_{33} + ab(\cos\gamma)\beta_{12} + ac(\cos\beta)\beta_{13} + bc(\cos\alpha)\beta_{23}]$.

Table 3. Selected Bond Distances (Å) and Angles (deg) for $(Et_4N)_3[Nb_2Cl_9]\cdot 5CH_2Cl_2$[a]

Nb–Nb′	2.7413(3)	Nb–Cl(2)′	2.513(1)
Nb–Cl(1)	2.513(1)	Nb–Cl(3)	2.443(1)
Nb′–Cl(1)	2.513(1)	Nb–Cl(4)	2.465(1)
Nb–Cl(2)	2.499(1)	Nb–Cl(5)	2.460(1)
Cl(1)–Nb–Cl(2)	92.70(3)	Cl(2)′–Nb–Cl(3)	89.93(4)
Cl(1)–Nb–Cl(2)′	92.37(3)	Cl(2)′–Nb–Cl(4)	177.56(4)
Cl(1)–Nb–Cl(3)	177.69(3)	Cl(2)′–Nb–Cl(5)	86.05(3)
Cl(1)–Nb–Cl(4)	86.39(3)	Cl(3)–Nb–Cl(4)	91.31(4)
Cl(1)–Nb–Cl(5)	89.80(3)	Cl(3)–Nb–Cl(5)	90.09(3)
Cl(2)–Nb–Cl(2)′	93.90(3)	Cl(4)–Nb–Cl(5)	91.85(3)
Cl(2)–Nb–Cl(3)	87.41(3)	Nb–Cl(1)–Nb′	66.10(3)
Cl(2)–Nb–Cl(4)	88.26(3)	Nb–Cl(2)–Nb′	66.31(3)
Cl(2)–Nb–Cl(5)	177.50(4)		

[a] Numbers in parentheses are estimated standard deviations in the least significant digits.

ions were required to be disordered and were poorly defined. Although the other possible space group *P62c* (No. 186) and possible subgroups, such as *P31c* (No. 163) and $P\bar{3}1c$ (No. 159), were all tried, the results were the same or worse. As a matter of fact, after several repetitions of data collection on different batches of crystals and repeated failure to solve completely the structure, an attempt was made to crystallize the compound in another crystal phase. However, this resulted in the above pentasolvate crystal structure.

X-ray Crystallography for $(Pr_4N)_3[Nb_2Cl_9]\cdot 6CH_2Cl_2$. These crystals were handled in the same way as the two above. Twenty-five reflections in the 2θ range 28–30° were used to refine the unit cell parameters. Three intensity standards were checked after every 2 h of crystal exposure, which revealed a total of 51.2% decay during a total of 85.5 h of exposure time. An anisotropic decay correction was applied to the intensity data along with other conventional corrections for Lorentz and polarization effects. An empirical absorption based on ψ scans of seven reflections was also applied. On the basis of the systematic absences, two space groups, *Iba2* (No. 45) and *Ibam* (No. 72), were possible. Since there were no significant peaks of the (0, 0, *w*) class (interatomic vectors generated by a mirror plane) in a three-dimensional Patterson map, while peaks of the (*u*, *v*, 0) class (created by a 2-fold axis) were significant, the space group *Iba2* was chosen. Positions of two independent Nb atoms were deduced from the Patterson map, and the remaining non-hydrogen

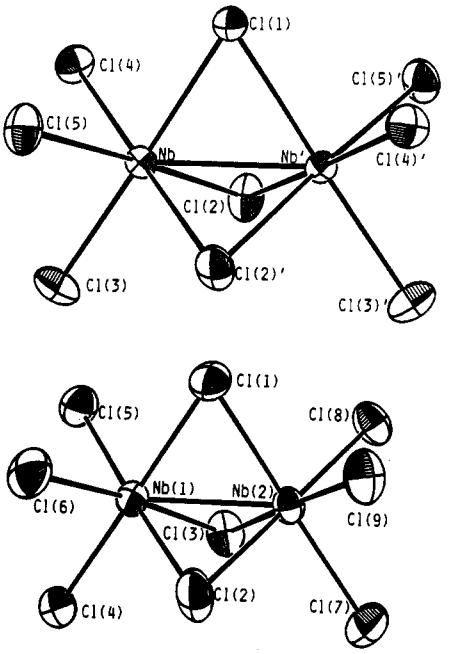

Figure 1. The $[Nb_2Cl_9]^{3-}$ ions found in two compounds: (a) upper, in the Et_4N^+ compound; (b) lower, in the Pr_4N^+ compound.

atoms were located successfully from least-squares refinements and difference Fourier syntheses. The final least-squares refinement, where all these non-hydrogen atoms were treated anisotropically, converged with $R_1 = 0.065$, $R_2 = 0.079$, and a goodness-of-fit indicator of 1.723 for 3554 intensity data with $F_o^2 > 3\sigma(F_o^2)$ and 612 variables. No effort was made to locate hydrogen atoms, since the quality of the data set was affected by a serious decay, as mentioned above. After the refinement was complete, a drawing of the unit cell contents showed no hidden mirror planes, which confirmed the choice of space group *Iba2*. The highest peak in a final difference Fourier map, 1.323 e/Å^3, was in the vicinity of the two Nb atoms along with the other first five peaks. Crystal data are listed in Table 1. Positional and equivalent isotropic thermal parameters of non-hydrogen atoms are listed in Table 4. Selected bond distances and angles are given in Table 5. The $[Nb_2Cl_9]^{3-}$ ion and its atom labels are shown in Figure 1b.

As we mentioned above, when the starting material $Nb_2Cl_6(THT)_3$ was used instead of $Nb_2Cl_6(Me_2S)_3$, another crystal phase was obtained. The cell parameters were determined to be as follows: $a = 17.219(2)$ Å, $b = 45.524(7)$ Å, $c = 18.410(2)$ Å, and $\alpha = \beta = \gamma = 90°$, which were only a little bit different. However, from the systematic absences the space group was determined uniquely to be *Pccn* (No. 56). This crystal sustained an even more severe intensity loss during the data collection process. Two intensity standards, (0,10,–11) and (–1,9,–3) dropped more than 60%, although the third one (912) had in fact no change at all. Considering that summations of the Miller indices $(h + k + l)$ for the first two standards were odd, while the value for the third was even, there was a possible phase transition from the primitive cell to the above body-centered cell. However, since the body-centered cell phase was also unstable, as shown by the more than 50% intensity loss, it remains uncertain if there really was a phase transition. Moreover, no solution of the structure was obtained. Much effort would be necessary to solve the problem of phase transitions in these crystals with such large dichloromethane content, and we have not pursued the matter further.

X-ray Crystallography for $(Et_4N)_2[Ta_2Cl_8(THT)]$. Crystals were examined by using the fritted-funnel device mentioned above in a stream of argon under a layer of mineral oil which was well degassed by stirring in a flask over Na threads on a vacuum line for at least 12 h. A crystal suitable for X-ray crystallography was then wedged in a thin-walled capillary, and the capillary was sealed in a flame. Orthorhombic unit cell parameters were refined by centering 25 reflections in the 2θ range 70–75° (Cu Kα radiation). There was no intensity loss during the data collection. On the basis of the observed systematic absences, the space group was determined uniquely to be *Pcca* (No. 54). Positions of the two independent Ta atoms and their coordinated atoms were located by direct methods.[11] The remaining non-hydrogen atoms were located in a succeeding difference Fourier synthesis. One tetraethylammonium cation was found to reside on a 2-fold axis with its four α-carbon atoms on two

Table 4. Positional and Equivalent Isotropic Thermal Parameters for $(Pr_4N)_3[Nb_2Cl_9]\cdot 6CH_2Cl_2$

atom	x	y	z	B_{eq},[a] Å^2
Nb(1)	0.18026(7)	0.86994(3)	0.500	2.72(3)
Nb(2)	0.29869(7)	0.87211(3)	0.59425(8)	2.61(3)
Cl(1)	0.1662(2)	0.8909(1)	0.6240(2)	4.0(1)
Cl(2)	0.2435(3)	0.82527(9)	0.5498(3)	5.5(1)
Cl(3)	0.3082(2)	0.8941(1)	0.4707(2)	3.64(9)
Cl(4)	0.1894(2)	0.8486(1)	0.3796(2)	4.1(1)
Cl(5)	0.1148(2)	0.9143(1)	0.4579(2)	4.1(1)
Cl(6)	0.0581(2)	0.8433(1)	0.5209(3)	4.8(1)
Cl(7)	0.4280(2)	0.8511(1)	0.5730(3)	4.4(1)
Cl(8)	0.3519(2)	0.91824(9)	0.6362(2)	3.87(9)
Cl(9)	0.2957(3)	0.8507(1)	0.7167(2)	4.2(1)
N(1)	0.2366(8)	−0.0043(3)	0.5450(8)	4.0(3)
C(1)	0.186(1)	0.0174(3)	0.502(1)	3.9(4)
C(2)	0.125(1)	0.0043(5)	0.453(1)	6.0(5)
C(3)	0.078(1)	0.0282(4)	0.422(1)	6.4(6)
C(4)	0.181(1)	−0.0244(4)	0.588(1)	5.0(4)
C(5)	0.128(1)	−0.0105(4)	0.639(1)	5.7(5)
C(6)	0.080(1)	−0.0303(5)	0.687(1)	8.8(7)
C(7)	0.286(1)	0.0139(4)	0.591(1)	4.5(4)
C(8)	0.345(1)	−0.0043(5)	0.637(1)	5.7(5)
C(9)	0.389(1)	0.0152(5)	0.685(1)	6.6(6)
C(10)	0.2807(9)	−0.0250(4)	0.4938(9)	3.7(4)
C(11)	0.341(1)	−0.0072(4)	0.445(1)	5.8(5)
C(12)	0.371(1)	−0.0298(5)	0.393(1)	6.8(6)
N(2)	0.0395(7)	0.3417(3)	0.3182(7)	4.0(3)
C(13)	0.048(1)	0.3738(4)	0.3185(9)	4.1(4)
C(14)	−0.006(1)	0.3920(4)	0.2702(9)	4.6(4)
C(15)	0.009(1)	0.4239(4)	0.283(1)	5.6(5)
C(16)	0.048(1)	0.3292(5)	0.236(1)	5.2(5)
C(17)	0.132(1)	0.3345(6)	0.206(1)	7.2(6)
C(18)	0.130(1)	0.3210(5)	0.129(1)	6.2(5)
C(19)	−0.0436(9)	0.3298(5)	0.3392(9)	5.2(5)
C(20)	−0.070(1)	0.3453(6)	0.408(1)	7.6(7)
C(21)	−0.154(1)	0.3337(5)	0.429(1)	7.0(6)
C(22)	0.099(1)	0.3269(4)	0.371(1)	5.4(5)
C(23)	0.102(1)	0.2933(6)	0.367(1)	8.9(7)
C(24)	0.168(2)	0.2798(7)	0.410(2)	13(1)
N(3)	0.0468(8)	0.1738(3)	0.2809(8)	4.3(3)
C(25)	0.054(1)	0.1839(4)	0.3559(9)	5.0(5)
C(26)	0.140(1)	0.1810(5)	0.387(1)	6.7(6)
C(27)	0.140(1)	0.1936(5)	0.464(1)	6.5(6)
C(28)	−0.0381(9)	0.1828(4)	0.263(1)	4.9(5)
C(29)	−0.063(1)	0.1719(6)	0.187(1)	8.0(7)
C(30)	−0.150(1)	0.1780(5)	0.180(1)	6.5(6)
C(31)	0.063(1)	0.1396(4)	0.275(1)	5.5(5)
C(32)	0.011(1)	0.1221(3)	0.322(1)	3.8(4)
C(33)	0.028(1)	0.0901(4)	0.309(1)	5.8(5)
C(34)	0.104(1)	0.1895(5)	0.227(1)	6.6(6)
C(35)	0.103(1)	0.2232(4)	0.231(1)	8.1(6)
C(36)	0.168(2)	0.2333(7)	0.191(2)	16(1)
C(37)	0.303(1)	0.4167(5)	0.295(1)	7.2(6)
Cl(10)	0.3327(4)	0.4555(1)	0.2859(3)	7.7(2)
Cl(11)	0.2330(4)	0.4108(2)	0.2286(4)	9.0(2)
C(38)	0.472(1)	0.0852(5)	0.549(2)	8.8(7)
Cl(12)	0.3770(4)	0.0955(2)	0.5695(4)	9.1(2)
Cl(13)	0.4755(4)	0.0521(2)	0.5052(5)	14.5(3)
C(39)	0.271(1)	0.0791(4)	0.301(1)	6.3(5)
Cl(14)	0.2647(7)	0.0420(2)	0.3000(4)	12.8(3)
Cl(15)	0.2718(9)	0.0917(2)	0.3853(5)	23.8(5)
C(40)	0.123(2)	0.2737(8)	0.622(2)	21.1(9)
Cl(16)	0.1040(5)	0.2658(2)	0.7204(5)	11.7(2)
Cl(17)	0.0512(8)	0.2596(3)	0.583(1)	21.3(5)
C(41)	0.372(1)	0.2754(5)	0.460(1)	8.7(7)
Cl(18)	0.3062(8)	0.2475(2)	0.5058(7)	19.1(4)
Cl(19)	0.4110(7)	0.2568(2)	0.4000(6)	22.7(3)
C(42)	0.075(1)	0.1022(6)	0.542(2)	12.4(9)
Cl(20)	0.0793(5)	0.0781(2)	0.6199(4)	11.3(2)
Cl(21)	0.1604(6)	0.1104(3)	0.5187(8)	21.7(4)

[a] Anisotropically refined atoms are given in the form of the equivalent isotropic displacement parameter defined as $(4/3)[a^2\beta_{11} + b^2\beta_{22} + c^2\beta_{33} + ab(\cos\gamma)\beta_{12} + ac(\cos\beta)\beta_{13} + bc(\cos\alpha)\beta_{23}]$.

sets of symmetry-related positions, as if the central nitrogen atom was enclosed in a cube formed by the eight carbon atoms. In the final least-squares refinement, bond length constraints were applied to this cation (N–C = 1.479 Å, C–C = 1.541 Å)[13] and these four α-carbon atoms were

Table 5. Selected Bond Distances (Å) and Angles (deg) for $(Pr_4N)_3[Nb_2Cl_9]\cdot 6CH_2Cl_2$[a]

Nb(1)–Nb(2)	2.691(2)	Nb(2)–Cl(1)	2.500(4)
Nb(1)–Cl(1)	2.506(4)	Nb(2)–Cl(2)	2.480(5)
Nb(1)–Cl(2)	2.490(5)	Nb(2)–Cl(3)	2.512(4)
Nb(1)–Cl(3)	2.524(4)	Nb(2)–Cl(7)	2.456(4)
Nb(1)–Cl(4)	2.447(4)	Nb(2)–Cl(8)	2.425(4)
Nb(1)–Cl(5)	2.445(5)	Nb(2)–Cl(9)	2.477(4)
Nb(1)–Cl(6)	2.461(4)		
Cl(1)–Nb(1)–Cl(2)	90.7(2)	Cl(1)–Nb(2)–Cl(7)	175.6(2)
Cl(1)–Nb(1)–Cl(3)	96.7(1)	Cl(1)–Nb(2)–Cl(8)	88.7(2)
Cl(1)–Nb(1)–Cl(4)	177.9(1)	Cl(1)–Nb(2)–Cl(9)	85.0(1)
Cl(1)–Nb(1)–Cl(5)	86.2(1)	Cl(2)–Nb(2)–Cl(3)	93.7(2)
Cl(1)–Nb(1)–Cl(6)	87.7(1)	Cl(2)–Nb(2)–Cl(7)	87.6(2)
Cl(2)–Nb(1)–Cl(3)	93.2(2)	Cl(2)–Nb(2)–Cl(8)	179.2(2)
Cl(2)–Nb(1)–Cl(4)	89.2(2)	Cl(2)–Nb(2)–Cl(9)	87.6(2)
Cl(2)–Nb(1)–Cl(5)	176.7(2)	Cl(3)–Nb(2)–Cl(7)	87.1(1)
Cl(2)–Nb(1)–Cl(6)	84.9(2)	Cl(3)–Nb(2)–Cl(8)	85.6(1)
Cl(3)–Nb(1)–Cl(4)	85.4(1)	Cl(3)–Nb(2)–Cl(9)	177.4(1)
Cl(3)–Nb(1)–Cl(5)	88.4(1)	Cl(7)–Nb(2)–Cl(8)	92.7(2)
Cl(3)–Nb(1)–Cl(6)	175.2(2)	Cl(7)–Nb(2)–Cl(9)	90.8(2)
Cl(4)–Nb(1)–Cl(5)	93.8(1)	Cl(8)–Nb(2)–Cl(9)	93.1(2)
Cl(4)–Nb(1)–Cl(6)	90.2(2)	Nb(1)–Cl(1)–Nb(2)	65.0(1)
Cl(5)–Nb(1)–Cl(6)	93.7(1)	Nb(1)–Cl(2)–Nb(2)	65.6(1)
Cl(1)–Nb(2)–Cl(2)	91.1(2)	Nb(1)–Cl(3)–Nb(2)	64.6(1)
Cl(1)–Nb(2)–Cl(3)	97.1(1)		

[a] Numbers in parentheses are estimated standard deviations in the least significant digits.

treated only isotropically, while all other non-hydrogen atoms were refined anisotropically. No further effort was made to locate hydrogen atoms, since the quality of the data set had been affected by this kind of partial structural disorder. Crystal data are listed in Table 1. Positional and equivalent isotropic thermal parameters are listed in Table 6. Selected bond distances and angles are given in Table 7. The $[Ta_2Cl_8(THT)]^{2-}$ ion is shown in Figure 2, along with the atom-labeling scheme. The disorder model for the tetraethylammonium cation is shown in a figure deposited as a part of the supplementary material.

X-ray Crystallography for $(Et_4N)_2[Nb_2Cl_8(THT)]$. The same crystallographic procedure as that for its Ta analogue was used. Since a different X-ray source (Mo Kα radiation) was used, reflections used to refine the unit cell parameters fell in the 2θ range 27–30°. Because of the isomorphism, atomic positions for the Ta analogue were directly used to begin refining the structure. There was the same disorder problem for a tetraethylammonium cation, but to a smaller extent. No bond length constraints were applied in the final least-squares refinement. Crystal data are listed in Table 1. Positional and equivalent isotropic thermal parameters are listed in Table 8. Selected bond distances and angles are given in Table 9. The atom-labeling scheme is the same as that shown in Figure 2 for the Ta analog.

Magnetic Measurements. The magnetic susceptibility measurements were carried out on crystalline samples of $(Bu_4N)[Nb_2Cl_7(PR_3)_2]$ and $(Et_4N)_2[Nb_2Cl_8(THT)]$.

Computational Procedures. The electronic structure calculations were performed for three ionic species, namely, $[Nb_2Cl_9]^{3-}$, $[Nb_2Cl_7(PH_3)_2]^-$, and $[Nb_2Cl_8SH_2]^{2-}$, where the last two are models for the $[Nb_2Cl_7(PR_3)_2]^-$ and $[Nb_2Cl_8(THT)]^{2-}$ ions in which the PR_3 and the tetrahydrothiophene ligands are replaced by PH_3 and SH_2, respectively. The structural parameters used in the calculations were all based on the crystal structures of the actual compounds but were idealized to ensure symmetries of D_{3h} for $[Nb_2Cl_9]^{3-}$ and C_{2v} for the two substituted compounds. The coordinate system used for all calculations is shown in Figure 3. Because it may later be useful to know the electronic structure of the $[Nb_2Cl_9]^{3-}$ ion when its symmetry is lowered to C_{2v}, such a calculation was also performed by the ab initio CI method. The C_{2v} symmetry of the ion was obtained by using a bond distance between an Nb atom and a terminal Cl atom at the X position (see Figure 3) 0.025 Å shorter than other four equivalent Nb–Cl(terminal) distances and assuming the dihedral angle Y–Nb–Nb–Cl(bridging) (see also Figure 3) to be 2.5° smaller than the angle Cl(bridging)–Nb–Nb–Cl(bridging). In D_{3h} symmetry, the Nb–Cl(terminal) distances are all the same and the dihedral angles are all 120°.

In SCF–Xα–SW calculations,[14a] the α values were taken from the compilation of Schwarz.[14b] Overlapping atomic spheres were used, and

(13) Sheldrick, G. M. SHELX-76: Program for X-ray Crystal Structure Determination. University of Cambridge, England, 1976.

Table 6. Positional and Equivalent Isotropic Thermal Parameters for $(Et_4N)_2[Ta_2Cl_8(THT)]$

atom	*x*	*y*	*z*	B_{eq},[a] Å^2
Ta(1)	0.16039(2)	0.22784(4)	0.11491(4)	3.65(1)
Ta(2)	0.09852(2)	0.24577(4)	−0.02095(4)	3.23(1)
Cl(1)	0.0801(1)	0.1833(2)	0.1333(2)	4.98(9)
Cl(2)	0.1202(1)	0.3630(2)	0.0842(2)	4.12(7)
Cl(3)	0.2321(1)	0.2981(2)	0.1041(3)	4.72(8)
Cl(4)	0.1856(1)	0.0923(3)	0.1588(3)	6.4(1)
Cl(5)	0.1567(2)	0.2682(3)	0.2819(3)	6.5(1)
Cl(6)	0.1146(1)	0.3295(2)	−0.1552(2)	4.73(8)
Cl(7)	0.0670(1)	0.1293(2)	−0.1014(3)	5.6(1)
Cl(8)	0.0218(1)	0.3078(2)	−0.0133(2)	4.64(8)
S	0.1714(1)	0.1849(2)	−0.0423(2)	3.55(7)
C(1)	0.2136(4)	0.2278(9)	−0.125(1)	4.8(4)
C(2)	0.2228(7)	0.158(1)	−0.195(1)	8.5(6)
C(3)	0.2047(9)	0.081(1)	−0.172(2)	12.4(9)
C(4)	0.1799(5)	0.0765(8)	−0.082(1)	4.7(3)
N(1)	0.250	0.500	0.342(1)	3.8(3)
C(5)	0.2757(6)	0.563(1)	0.401(1)	6.4(4)
C(6)	0.3135(7)	0.519(1)	0.460(2)	9.5(7)
C(7)	0.2837(5)	0.449(1)	0.281(1)	5.9(4)
C(8)	0.3144(7)	0.504(1)	0.218(1)	8.5(6)
N(2)	0.5978(3)	0.1506(7)	0.4629(8)	4.6(3)
C(9)	0.5969(5)	0.244(1)	0.488(1)	6.2(5)
C(10)	0.6106(7)	0.302(1)	0.411(1)	8.2(6)
C(11)	0.5887(5)	0.101(1)	0.552(1)	6.4(5)
C(12)	0.5432(6)	0.118(1)	0.597(2)	9.1(6)
C(13)	0.5598(5)	0.140(1)	0.388(1)	7.2(5)
C(14)	0.5553(6)	0.048(1)	0.362(1)	7.6(5)
C(15)	0.6437(5)	0.124(1)	0.421(1)	7.1(5)
C(16)	0.6830(6)	0.143(1)	0.485(2)	8.6(6)
N(3)	0.500	0.4797(9)	0.750	4.2(4)
C(17)	0.5234(7)	0.5567(8)	0.780(2)	5.1(6)[b]
C(18)	0.500	0.638(1)	0.750	6.5(6)
C(19)	0.5225(8)	0.4018(8)	0.780(2)	5.9(7)[b]
C(20)	0.500	0.319(1)	0.750	7.9(8)
C(21a)	0.4526(2)	0.477(2)	0.783(1)	5.8(7)[b]
C(21b)	0.5011(5)	0.481(2)	0.6467(2)	4.8(6)[b]
C(22)	0.4501(5)	0.475(1)	0.891(1)	9.3(7)

[a] Anisotropically refined atoms are given in the form of the equivalent isotropic displacement parameter defined as $(4/3)[a^2\beta_{11} + b^2\beta_{22} + c^2\beta_{33} + ab(\cos\gamma)\beta_{12} + ac(\cos\beta)\beta_{13} + bc(\cos\alpha)\beta_{23}]$. [b] Atoms were refined isotropically.

Table 7. Selected Bond Distances (Å) and Angles (deg) for $(Et_4N)_2[Ta_2Cl_8(THT)]$[a]

Ta(1)–Ta(2)	2.6875(8)	Ta(2)–Cl(1)	2.488(4)
Ta(1)–Cl(1)	2.493(3)	Ta(2)–Cl(2)	2.494(3)
Ta(1)–Cl(2)	2.512(3)	Ta(2)–Cl(6)	2.395(4)
Ta(1)–Cl(3)	2.408(3)	Ta(2)–Cl(7)	2.386(4)
Ta(1)–Cl(4)	2.384(4)	Ta(2)–Cl(8)	2.480(3)
Ta(1)–Cl(5)	2.481(4)	Ta(2)–S	2.386(3)
Ta(1)–S	2.378(3)		
Cl(1)–Ta(1)–Cl(2)	79.4(1)	Cl(1)–Ta(2)–Cl(7)	91.6(1)
Cl(1)–Ta(1)–Cl(3)	168.6(1)	Cl(1)–Ta(2)–Cl(8)	85.6(1)
Cl(1)–Ta(1)–Cl(4)	90.5(1)	Cl(1)–Ta(2)–S	98.4(1)
Cl(1)–Ta(1)–Cl(5)	86.0(1)	Cl(2)–Ta(2)–Cl(6)	90.6(1)
Cl(1)–Ta(1)–S	98.5(1)	Cl(2)–Ta(2)–Cl(7)	169.5(1)
Cl(2)–Ta(1)–Cl(3)	90.1(1)	Cl(2)–Ta(2)–Cl(8)	84.6(1)
Cl(2)–Ta(1)–Cl(4)	169.1(1)	Cl(2)–Ta(2)–S	98.9(1)
Cl(2)–Ta(1)–Cl(5)	85.6(1)	Cl(6)–Ta(2)–Cl(7)	97.4(1)
Cl(2)–Ta(1)–S	98.6(1)	Cl(6)–Ta(2)–Cl(8)	89.6(1)
Cl(3)–Ta(1)–Cl(4)	99.7(1)	Cl(6)–Ta(2)–S	87.0(1)
Cl(3)–Ta(1)–Cl(5)	88.8(1)	Cl(7)–Ta(2)–Cl(8)	88.8(1)
Cl(3)–Ta(1)–S	87.4(1)	Cl(7)–Ta(2)–S	88.3(1)
Cl(4)–Ta(1)–Cl(5)	89.9(1)	Cl(8)–Ta(2)–S	175.1(1)
Cl(4)–Ta(1)–S	86.7(1)	Ta(1)–Cl(1)–Ta(2)	65.31(9)
Cl(5)–Ta(1)–S	174.4(1)	Ta(1)–Cl(2)–Ta(2)	64.95(8)
Cl(1)–Ta(2)–Cl(2)	79.8(1)	Ta(1)–S–Ta(2)	68.68(9)
Cl(1)–Ta(2)–Cl(6)	169.6(1)		

[a] Numbers in parentheses are estimated standard deviations in the least significant digits.

their radii were chosen to be 89% of the atomic number radii.[14c] A Watson sphere[14d] with the same radius as that of the outer sphere which touches the outermost atomic sphere and with opposite charges was used for each of the ionic compounds.

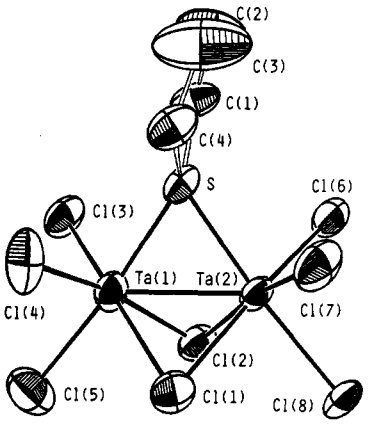

Figure 2. The $[Ta_2Cl_8(THT)]^{2-}$ ion and the atom-labeling scheme. A corresponding labeling scheme is used for the isomorphous niobium compound.

Table 8. Positional and Equivalent Isotropic Thermal Parameters for $(Et_4N)_2[Nb_2Cl_8(THT)]$

atom	*x*	*y*	*z*	B_{eq},[a] Å^2
Nb(1)	0.16075(4)	0.22722(8)	0.11586(9)	3.13(3)
Nb(2)	0.09820(4)	0.24598(8)	−0.02019(9)	2.78(2)
Cl(1)	0.0807(1)	0.1809(3)	0.1335(3)	4.48(9)
Cl(2)	0.1209(1)	0.3620(2)	0.0850(3)	3.61(8)
Cl(3)	0.2328(1)	0.2973(2)	0.1039(3)	4.17(9)
Cl(4)	0.1865(2)	0.0901(3)	0.1569(3)	5.6(1)
Cl(5)	0.1577(2)	0.2665(3)	0.2841(3)	5.8(1)
Cl(6)	0.1146(1)	0.3296(3)	−0.1558(3)	4.41(9)
Cl(7)	0.0671(1)	0.1280(2)	−0.1024(3)	5.0(1)
Cl(8)	0.0212(1)	0.3080(2)	−0.0124(3)	4.10(9)
S	0.1717(1)	0.1839(2)	−0.0436(3)	3.00(8)
C(1)	0.2136(5)	0.2265(9)	−0.127(1)	3.9(3)
C(2)	0.2233(7)	0.157(1)	−0.194(1)	8.8(6)
C(3)	0.2036(8)	0.082(1)	−0.170(1)	10.2(6)
C(4)	0.1794(5)	0.0745(8)	−0.082(1)	4.3(4)
N(1)	0.250	0.500	0.343(1)	3.8(4)
C(5)	0.2756(6)	0.5652(9)	0.402(1)	5.1(4)
C(6)	0.3123(6)	0.521(1)	0.460(1)	9.0(6)
C(7)	0.2839(6)	0.4483(9)	0.285(1)	5.4(4)
C(8)	0.3162(7)	0.502(1)	0.221(1)	8.6(5)
N(2)	0.5970(4)	0.1507(7)	0.4634(8)	3.9(3)
C(9)	0.5975(6)	0.245(1)	0.488(1)	5.6(4)
C(10)	0.6120(7)	0.304(1)	0.409(1)	6.7(5)
C(11)	0.5876(6)	0.103(1)	0.554(1)	6.1(5)
C(12)	0.5431(6)	0.120(1)	0.599(1)	8.1(6)
C(13)	0.5596(6)	0.141(1)	0.389(1)	6.9(5)
C(14)	0.5536(7)	0.046(1)	0.364(2)	8.5(6)
C(15)	0.6431(6)	0.124(1)	0.426(1)	6.6(5)
C(16)	0.6830(5)	0.142(1)	0.485(1)	6.6(5)
N(3)	0.500	0.478(1)	0.750	4.3(4)
C(17)	0.526(1)	0.557(2)	0.782(2)	5.1(8)
C(18)	0.500	0.643(1)	0.750	7.0(7)
C(19)	0.5257(9)	0.403(2)	0.779(2)	4.9(7)
C(20)	0.500	0.319(1)	0.750	7.0(8)
C(21a)	0.448(1)	0.478(2)	0.771(2)	3.8(7)[b]
C(21b)	0.501(1)	0.482(2)	0.633(2)	5.1(8)[b]
C(22)	0.4481(8)	0.475(1)	0.894(2)	2.3(5)[b]

[a] Anisotropically refined atoms are given in the form of the equivalent isotropic displacement parameter defined as $(4/3)[a^2\beta_{11} + b^2\beta_{22} + c^2\beta_{33} + ab(\cos\gamma)\beta_{12} + ac(\cos\beta)\beta_{13} + bc(\cos\alpha)\beta_{23}]$. [b] Atoms were refined isotropically.

The ab initio CI calculations utilized effective core potentials (ECP) so that only the outermost electrons of each atom were treated explicitly. For niobium, these include electrons in 4s, 4p, 4d, and 5s orbitals, and for chlorine, sulfur, and phosphorus these are the 3s and 3p electrons. We used the ECPs of Hay and Wadt and their valence Gaussian basis set.[15]

(14) (a) Slater, J. C. *Quantum Theory of Molecules and Solids*; McGraw-Hill: New York, 1974; Vol. IV. (b) Schwarz, K. *Phys. Rev. B* **1972**, *5*, 2466. (c) Norman, J. G., Jr. *Mol. Phys.* **1976**, *31*, 1191. (d) Watson, R. E. *Phys. Rev.* **1958**, *111*, 1108.
(15) Hay, P. J.; Wadt, W. R. *J. Chem. Phys.* **1985**, *82*, 270, 284, 299.

Table 9. Selected Bond Distances (Å) and Angles (deg) for $(Et_4N)_2[Nb_2Cl_8(THT)]$[a]

Nb(1)–Nb(2)	2.707(2)	Nb(2)–Cl(1)	2.494(4)
Nb(1)–Cl(1)	2.498(4)	Nb(2)–Cl(2)	2.489(4)
Nb(1)–Cl(2)	2.504(4)	Nb(2)–Cl(6)	2.412(4)
Nb(1)–Cl(3)	2.418(4)	Nb(2)–Cl(7)	2.413(4)
Nb(1)–Cl(4)	2.403(4)	Nb(2)–Cl(8)	2.490(4)
Nb(1)–Cl(5)	2.496(4)	Nb(2)–S	2.417(4)
Nb(1)–S	2.412(4)		
Cl(1)–Nb(1)–Cl(2)	80.1(1)	Cl(1)–Nb(2)–Cl(7)	91.3(1)
Cl(1)–Nb(1)–Cl(3)	169.5(1)	Cl(1)–Nb(2)–Cl(8)	86.4(1)
Cl(1)–Nb(1)–Cl(4)	90.2(2)	Cl(1)–Nb(2)–S	97.9(1)
Cl(1)–Nb(1)–Cl(5)	86.7(1)	Cl(2)–Nb(2)–Cl(6)	91.0(1)
Cl(1)–Nb(1)–S	97.9(1)	Cl(2)–Nb(2)–Cl(7)	170.5(1)
Cl(2)–Nb(1)–Cl(3)	90.1(1)	Cl(2)–Nb(2)–Cl(8)	85.5(1)
Cl(2)–Nb(1)–Cl(4)	169.9(2)	Cl(2)–Nb(2)–S	98.6(1)
Cl(2)–Nb(1)–Cl(5)	86.3(1)	Cl(6)–Nb(2)–Cl(7)	96.9(1)
Cl(2)–Nb(1)–S	98.4(1)	Cl(6)–Nb(2)–Cl(8)	89.9(1)
Cl(3)–Nb(1)–Cl(4)	99.4(2)	Cl(6)–Nb(2)–S	86.3(1)
Cl(3)–Nb(1)–Cl(5)	89.0(2)	Cl(7)–Nb(2)–Cl(8)	89.2(1)
Cl(3)–Nb(1)–S	87.0(1)	Cl(7)–Nb(2)–S	87.2(1)
Cl(4)–Nb(1)–Cl(5)	90.4(2)	Cl(8)–Nb(2)–S	174.5(1)
Cl(4)–Nb(1)–S	85.7(1)	Nb(1)–Cl(1)–Nb(2)	65.7(1)
Cl(5)–Nb(1)–S	173.9(1)	Nb(1)–Cl(2)–Nb(2)	65.7(1)
Cl(1)–Nb(2)–Cl(2)	80.4(1)	Nb(1)–S–Nb(2)	68.2(1)
Cl(1)–Nb(2)–Cl(6)	170.9(1)		

[a] Numbers in parentheses are estimated standard deviations in the least significant digits.

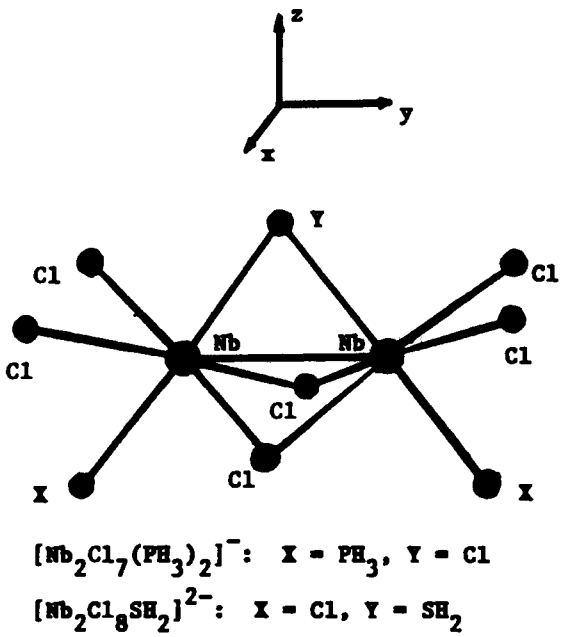

Figure 3. Model compounds and coordinate system used in the calculations.

For Nb, the (5s5p4d) basis set was contracted to a (3s3p3d) basis set, which gives rise to a d basis of triple-ζ quality. For Cl, S, and P, the (3s3p) basis set was contracted to a double-ζ (2s2p) set. For hydrogen, while a single-ζ basis function consisting a set of four primitive Gaussian functions of Huzinaga[16] was used in the calculations for $[Nb_2Cl_7(PH_3)_2]^-$, the (4s) set was contracted to a double-ζ (2s) set for the calculations on $[Nb_2Cl_8SH_2]^{2-}$.

Our multireference CI calculations followed the procedure of Benard and coworkers.[17] It was designed for calculations on the types of metal–metal-bonded binuclear complexes in which the metal–metal interaction may be coupled with the metal–ligand interaction, and thus a balanced description of these interactions is required. The set of orbitals used for CI expansions in such calculations is a set of natural orbitals and is optimized through a two-step single-reference CI procedure.[17]

From the set of optimized orbitals, a single-reference CI calculation for each state of interest was carried out first in order to determine the most important configurations for the following multireference CI calculation. All configurations with coefficients $|c| \geq 0.1$ were taken as references in the following multireference CI treatment. If additional configurations fulfilling the same condition appeared in the CI expansion list of the multireference CI, as is the case in general, they were then added to the reference list and an additional multireference CI calculation was performed to obtain the final result.

All ab initio calculations were carried with the GAMESS program[18] either on a CRAY Y-MP2 computer at the Texas A&M University Supercomputer Center or on a FPS E-522 computer in the Department of Chemistry of Texas A&M University.

Results and Discussion

The Isomorphous $(Et_4N)_2[M_2Cl_8(THT)]$ Compounds. The two anions have almost identical dimensions. Moreover, as can be seen in Table 10, these anions, in which the only R_2S ligand is the one in the bridging position, display no important structural differences from the molecular species in which there are also two terminal neutral ligands occupying positions trans to the μ-THT or μ-Me_2S ligand.

The $[Nb_2Cl_9]^{3-}$ Ion. The only previous structural characterization of this species was in the compound $Cs_3Nb_2Cl_9$.[1] Because of the well-known fact[19] that the Mo–Mo distances in compounds of the $[Mo_2Cl_9]^{3-}$ ion vary considerably with changes in the accompanying cations, and tend to be particularly short in the tightly packed compounds in which the cations are small alkali metal ions, we considered it important to characterize the $[Nb_2Cl_9]^{3-}$ ion in several additional compounds especially those with "soft" cations that would tend to place minimal constraints on its dimensions. As described in the Experimental Section, several such compounds were prepared and examined, but only for two, namely, $(Et_4N)_3[Nb_2Cl_9]\cdot 5CH_2Cl_2$ and $(Pr_4N)_3[Nb_2Cl_9]\cdot 6CH_2Cl_2$, were satisfactorily accurate dimensions obtained. The Nb–Nb distances found, 2.74 and 2.69 Å, respectively, bracket the value previously[1] reported for $Cs_3Nb_2Cl_9$.

The Et_4N^+ compound was used for the magnetic measurements, and the details of its structure also enter into the interpretation of the magnetic properties; therefore a few comments on these structural details are warranted. The $[Nb_2Cl_9]^{3-}$ ion in this crystal resides on a crystallographic 2-fold axis that passes through one bridging chlorine atom and is therefore not required to conform to any symmetry higher than C_2. In fact, it comes close to having D_{3h} symmetry, as might have been expected. The three crystallographically independent Nb–Cl_t distances are all in the range 2.443(1)–2.465(1) Å, and the three independent Nb–Cl_b distances are in the range 2.499(1)–2.513(1) Å. Similarly, the three independent Cl_t–Nb–Cl_t' angles vary only from 90.09(3) to 91.85(3)° and the three Cl_b–Nb–Cl_b angles are in the range 92.37(3)–93.90(3)°. However, the deviations from D_{3h} symmetry do show some tendency toward C_{2v} symmetry, since the Nb–Cl(4) and Nb–Cl(5) distances are virtually the same at the 3σ level, while the Nb–Cl(3) distance is significantly shorter than their average (i.e., by 16σ). Similarly, the Cl(2)–Nb–Cl(2)′ angles are 93.90(3)° while the two independent Cl(1)–Nb–Cl(2) and Cl(1)–Nb–Cl(2)′ angles are closer to each other, viz., 92.70(3) and 92.37(3)°.

Electronic Structure by SCF–Xα–SW Calculations. The results of the SCF–Xα–SW calculations for the three face-sharing compounds are shown in Figure 4. The molecular orbitals shown are only the highest occupied and lowest unoccupied orbitals. All these MOs have predominant contributions (at least 75%) from the metal atoms and are pertinent to the metal–metal interaction. Other occupied MOs for each compound that are not listed and

(16) Huzinaga, S. *J. Chem. Phys.* **1965**, *42*, 1293.
(17) Poumbga, C.; Daniel, C.; Benard, M. *J. Am. Chem. Soc.* **1991**, *113*, 1090.
(18) Guest, M. F. *GAMESS User's Guide and Reference Manual*; Daresbury Laboratory: Daresbury, U.K., 1989.
(19) Stranger, R.; Smith, P. W.; Grey, I. E. *Inorg. Chem.* **1989**, *28*, 1271.

Table 10. Important Bond Distances (Å) for Face-Sharing Bioctahedral Compounds of Niobium and Tantalum

	M–M	M–X_b	M–S_b	M–X_t[a]	M–$X_{t'}$[a]	ref
$(Et_4N)_2[Nb_2Cl_8(THT)]$	2.707(2)	2.496[3]	2.413[3]	2.412[3]	2.493[3]	this work
$(Et_4N)_2[Ta_2Cl_8(THT)]$	2.688(1)	2.497[5]	2.382[4]	2.393[5]	2.480[1]	this work
$(Et_4N)_3[Nb_2Cl_9]$	2.7413(3)	2.508[5]		2.456[7]		this work
$(Pr_4N)_3[Nb_2Cl_9]$	2.691(2)	2.502[7]		2.452[7]		this work
$Cs_3Nb_2Cl_9$	2.70(1)					1
$Nb_2Cl_6(Me_2S)(THF)_2$	2.684(2)	2.489[2]	2.406[1]	2.375[5]	2.234[1]	2
$Ta_2Cl_6(Me_2S)(THF)_2$	2.6695(5)	2.494[1]	2.370[1]	2.368[1]	2.229[10]	2
$Ta_2Cl_6(Me_2S)_3$	2.691(1)	2.50[2]	2.378[5]	2.372[7]	2.618[5]	7a
$Ta_2Cl_6(THT)_3$	2.681(1)	2.503[9]	2.390[1]	2.366[4]	2.629[7]	7a
$(Bu_4N)[Nb_2Cl_7(PMe_3)_2]$	2.683(1)	2.51[1]		2.404[7]		6
$(Bu_4N)[Nb_2Cl_7(PEt_3)_2]$	2.708(3)	2.50[1]		2.45[5]		6

[a] X_t = terminal X trans to bridging X (X_b); $X_{t'}$ = terminal ligand trans to bridging S (S_b).

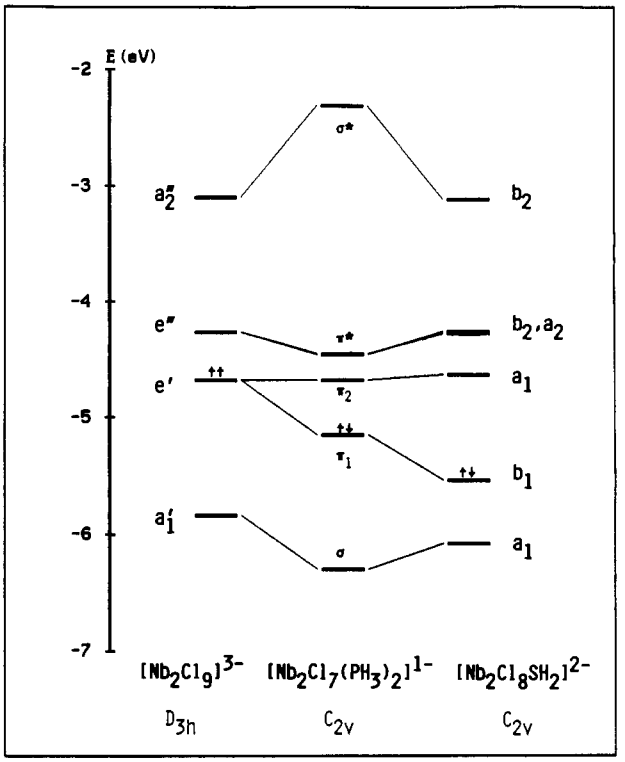

Figure 4. Molecular orbital diagrams for the three face-sharing compounds from the SCF–Xα–SW calculations.

have lower energies represent metal–ligand bonding, bonding within the ligands, or ligand lone pairs.

Before we look at the calculation in more detail, let us see how the electronic structure of the face-sharing compounds may be described in a simple and qualitative way. Consider an octahedral NbX_6 portion of the dinuclear unit with one 3-fold axis of the octahedron as the axis of quantization. Neglecting two d orbitals of the metal atom involved in Nb–X σ bonding and any π interactions with the ligands, there are three d orbitals (one dσ and two dπ orbitals) available to hold metal d electrons. Two such octahedra can be fused on a common triangular face in a way that gives rise to a molecular structure of D_{3h} symmetry, as in the case of $[Nb_2Cl_9]^{3-}$. Therefore, two dσ orbitals can overlap to form σ and σ* molecular orbitals, whose symmetry designations would be a_1' and a_2'', respectively. In addition, the dπ orbitals from the two octahedra can interact to form degenerate bonding and antibonding molecular orbitals, with symmetry designations e′ and e″, respectively. For $[Nb_2Cl_9]^{3-}$ with only four metal d electrons, an open-shell electronic configuration with two unpaired electrons, $(a_1')^2(e')^2$, should then result. The molecular symmetry would be reduced to C_{2v} in $[Nb_2Cl_7(PR_3)_2]^-$ and $[Nb_2Cl_8(\mu\text{-THT})]^{2-}$ as a result of the replacements of ligands at the terminal and bridging positions, respectively, and the degenerate orbitals of $[Nb_2Cl_9]^{3-}$ would split. The unpaired electrons would then occupy the bonding MO of lower energy and become paired. Therefore, the compounds of C_{2v} symmetry could have a singlet ground state derived from the closed-shell electronic configuration.

This qualitative picture agrees with the electronic structure calculated by the Xα method as shown in Figure 4. For $[Nb_2Cl_9]^{3-}$, the HOMO, the e′ orbital, is only half-filled and has metal–metal bonding character of π type. The LUMO is the antibonding counterpart of the HOMO and belongs to the e″ representation of the molecular point group. It may be noted that the HOMO–LUMO energy gap is rather small, namely, 0.4 eV. The contour plots of the e′ and e″ orbitals are shown in Figure 5. It can be seen that they are actually hybridizations of the π- and δ-type orbitals that, in the case of quadruply bonded systems with 4-fold symmetries, remain distinct. Even though we refer to the metal–metal bonding shown in Figure 5 as π bonding, it is apparently weaker than the π bonding that occurs in molecules with metal–metal quadruple bonds. The σ-type bonding and antibonding orbitals as calculated are the a_1' and a_2'' orbitals in Figure 4, respectively. The qualitative conclusion, however, is that the metal–metal interaction in $[Nb_2Cl_9]^{3-}$ can be formally described as a Nb–Nb double bond.

From $[Nb_2Cl_9]^{3-}$ to $[Nb_2Cl_7(PH_3)_2]^-$ and $[Nb_2Cl_8SH_2]^{2-}$, we can track increasing splitting of the degenerate e′ orbital into a b_1 (π_1) and an a_1 (π_2) orbital (see Figure 4). With the double occupation of the lower Nb–Nb bonding b_1 orbital, a singlet ground state is, therefore, well defined for both $[Nb_2Cl_7(PH_3)_2]^-$ and $[Nb_2Cl_8SH_2]^{2-}$. It is interesting to see that the replacement of a bridging chlorine atom by a thioether ligand has effects on the electronic structure very different from those due to the replacement at terminal positions by phosphine ligands. This is most clearly indicated by a much larger splitting of the e′ orbital and thus a comparatively larger HOMO–LUMO gap in the thioether compound. As in the case of $[Nb_2Cl_9]^{3-}$, a metal–metal bonding interaction is indicated, and the Nb–Nb bond in these two compounds of C_{2v} symmetry can also be formally assigned as a double bond. The similar natures of the metal–metal interactions as revealed by the molecular orbital calculations in all these compounds are consistent with the fact that the Nb–Nb bond distances in them are very similar.

Electronic Structure by ab Initio CI Calculations. The energy diagram obtained by the multireference CI calculations is shown in Figure 6, where the ground state and a few lowest excited states are listed for each of the three face-sharing compounds. The $[Nb_2Cl_9]^{3-}$ ion has been calculated in both D_{3h} and C_{2v} symmetries. While it is certainly appropriate to study the electronic structure of this compound by assuming the ideal D_{3h} molecular symmetry, deviation of the crystalline compound from the D_{3h} symmetry may need to be considered in the study of magnetic properties of the compound. However, this matter will not be pursued further at present.

For $[Nb_2Cl_9]^{3-}$ considered in D_{3h} symmetry, the ground-state electronic configuration, $(e')^2$ or π^2, gives rise to three electronic states, namely, $^3A_2'$, $^1E'$, and $^1A_1'$. There are six electronic states from the $(e'e'')^2$ configuration, namely, A_1'', A_2'', and E'', each of which can be either a spin singlet or a spin triplet. As shown

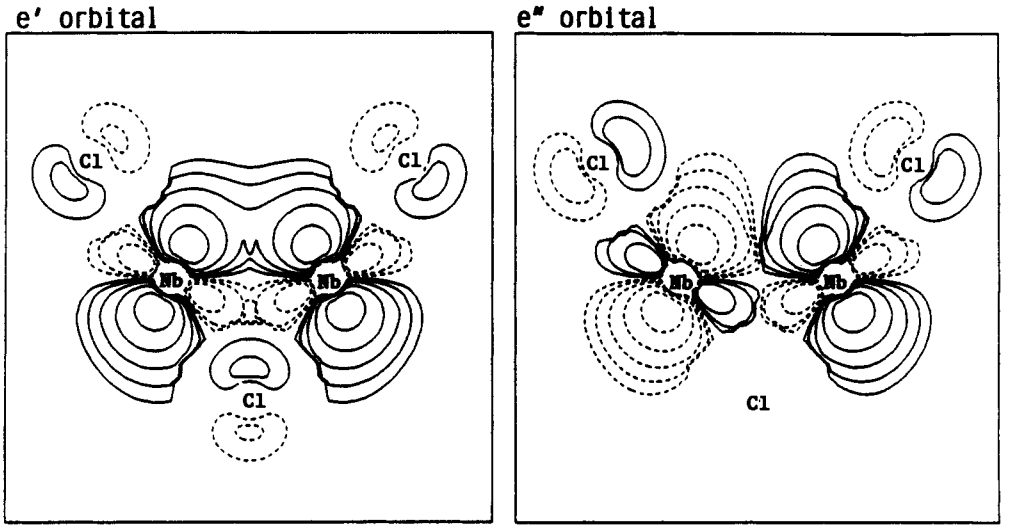

Figure 5. Molecular orbital contour plots for the e′ and e″ orbitals of $[Nb_2Cl_9]^{3-}$ from the SCF–Xα–SW calculations.

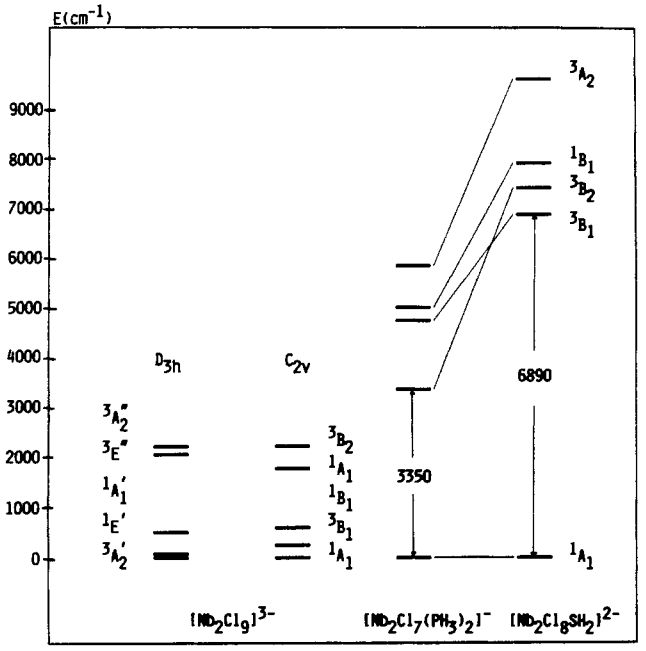

Figure 6. Total electronic energy diagrams for the three face-sharing compounds from the ab initio multireference CI calculations.

in the first column of Figure 6, the calculated ground state of the D_{3h} $[Nb_2Cl_9]^{3-}$ compound is the triplet state, $^3A_2'$, as would be expected for a system with two unpaired electrons. It is noteworthy that the electronic states derived from the $(e')^2$ configuration are very closely spaced. Thus, the ground state is only slightly below the next doubly degenerate singlet $^1E'$ state (with a predicted energy difference of only 80 cm^{-1}), and the second lowest excited state, the singlet $^1A_1'$ state, is separated from the ground state by only 500 cm^{-1}. Considering the accuracy that may be expected for the calculations reported here, we are not going to attach any quantitative significance to an energy value as small as 80 cm^{-1}. But we want to emphasize that the qualitative features of the calculated electronic structure are very important to the understanding of the magnetic properties of the compound, as we will see later. Consistent with the Xα molecular orbital calculations, a formal double bond between the metal atoms was also predicted by the CI calculations. This may be best illustrated by the populations of the relevant natural orbitals in the ground state, namely, $\sigma^{1.79}\pi^{1.50}\pi^{*0.50}\sigma^{*0.20}$.

The results of the CI calculations for $[Nb_2Cl_9]^{3-}$ in C_{2v} symmetry are shown in the second column in Figure 6. The lowest four electronic states directly correlate to the lowest three states of the same compound calculated in D_{3h} symmetry, as would be expected. Notably, in C_{2v} symmetry, the ground state is the singlet $^1A_1$ state, apparently as a result of splitting of the $^1E'$ state of the D_{3h} symmetry. The other component of the $^1E'$ state gives rise to the $^1B_1$ state. Similarly, we have now the $^3B_1$ state and another $^1A_1$ state which are from the $^3A_2'$ and $^1A_1'$ states upon lowering symmetry, respectively. The triplet and singlet B_1 states are respectively 250 and 590 cm^{-1} higher in energy than the $^1A_1$ ground state, and the next higher $^1A_1$ state is 1770 cm^{-1} above the ground state.

Let us now turn to the results of the CI calculations for $[Nb_2Cl_7(PH_3)_2]^-$ and $[Nb_2Cl_8SH_2]^{2-}$, also illustrated in Figure 6. Clearly, the electronic structures of these two ionic compounds, both having pronounced C_{2v} symmetry, are very different from that of $[Nb_2Cl_9]^{3-}$. We see again, as predicted by the Xα MO calculations, that changes of the ligands in the bridging or in the terminal positions can have strong effects on the electronic structure of the face-sharing bioctahedral compounds. In both $[Nb_2Cl_7(PH_3)_2]^-$ and $[Nb_2Cl_8SH_2]^{2-}$ the ground state is the same singlet $^1A_1$ state derived from the closed-shell configuration $(a_1)^2(b_1)^2$ or $\sigma^2\pi_1^2$, which is the leading configuration in the final CI wave function. The populations of the metal–metal bonding and antibonding natural orbitals in the ground state are as follows: $\sigma^{1.81}\pi_1^{1.50}\pi_1^{*0.48}\sigma^{*0.18}$ for $[Nb_2Cl_7(PH_3)_2]^-$ and $\sigma^{1.84}\pi_1^{1.71}\pi_1^{*0.27}\sigma^{*0.15}$ for $[Nb_2Cl_8SH_2]^{2-}$.

The predicted energy difference between the ground state and the first excited state is 3350 cm^{-1} in $[Nb_2Cl_7(PH_3)_2]^-$. Such a difference is large enough to prevent any significant thermal population of the triplet excited state at or below room temperature. The corresponding energy difference is doubled in the case of $[Nb_2Cl_8SH_2]^{2-}$. The large increase in this energy difference, from $[Nb_2Cl_7(PH_3)_2]^-$ to $[Nb_2Cl_8SH_2]^{2-}$, parallels the change in the HOMO–LUMO energy gap which was seen in the Xα MO calculations. As may be noted, the first excited state in the phosphine compound is the $^3B_2$ state corresponding to an electronic configuration $\pi_1^1\pi_1^{*1}$, instead of the $^3B_1$ state corresponding to the $\pi_1^1\pi_2^1$ configuration as would be expected. This, however, should not be very surprising since the antibonding π_1^* orbital is only a little higher in energy than the bonding π_2 orbital, as shown by the results of the Xα calculations in Figure 4. It has been reported[5] that the lowest absorption band occurs at 9700 cm^{-1} in the electronic absorption spectrum of $[Nb_2Cl_8(THT)]^{2-}$. This may be compared with the calculated energy, 7910 cm^{-1}, for the lowest dipole- and spin-allowed $^1B_1 \leftarrow {}^1A_1$ transition (see Figure 6) in the model compound $[Nb_2Cl_8SH_2]^{2-}$. Considering the difference between the model and actual compounds and the fact that the calculated energy is

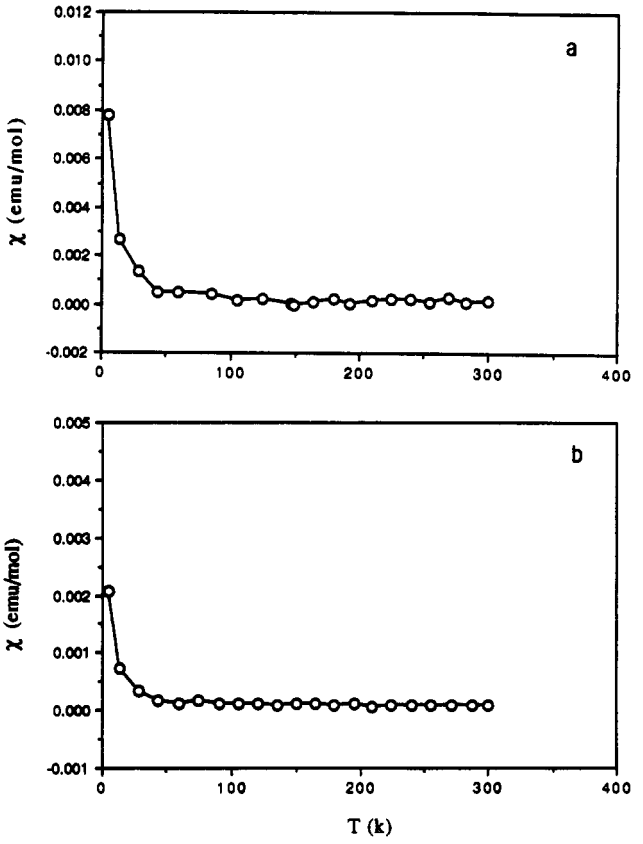

Figure 7. Plots of measured magnetic molar susceptibilities versus temperature, after diamagnetic corrections made by Pascal's constants, for (a) $(Bu_4N)[Nb_2Cl_7(PEt_3)_2]$ and (b) $(Et_4N)_2[Nb_2Cl_8(THT)]$.

simply for a vertical transition, the agreement should be considered acceptable.

Finally, we would emphasize that the results of our CI calculations confirm again the existence of strong metal–metal bonding interactions in these face-sharing bioctahedral compounds. As has been indicated clearly by the populations of the relevant natural orbitals, each of the metal–metal interactions can be formally described as a double bond between the two niobium atoms.

Magnetic Properties of the Face-Sharing Compounds. In the original report[1] on the $Cs_3Nb_2X_9$ ions (X = Cl, Br, I), magnetic measurements appeared to suggest that there are two unpaired electrons in the $[Nb_2X_9]^{3-}$ ions, which would be consistent with the expected open-shell $\sigma^2\pi^2$ configuration, but the very large Weiss constants make a simple interpretation doubtful. In a later study by Maas and McCarley,[5] magnetic susceptibilities of some face-sharing niobium(III) compounds were measured at a few points in a temperature range from 77 to 297 K. It was found that, although paramagnetic, the susceptibilities of $(Et_4N)_3[Nb_2Cl_9]$ are low and the corresponding magnetic moments are far below the expectation for two unpaired electrons. Moreover, the susceptibilities were reported to be almost temperature independent. The same authors also reported temperature-independent paramagnetism for two other compounds, namely, $Nb_2Cl_6(THT)_3$ and $(Et_4N)_2[Nb_2Cl_8(THT)]$. We report here the results of magnetic measurements on three face-sharing bioctahedral niobium compounds over a wide temperature range, namely, from about 5 to 300 K for $(Bu_4N)[Nb_2Cl_7(PEt_3)_2]$ and $(Et_4N)_2[Nb_2Cl_8(THT)]$ and from 9.7 to 304.2 K for $(Et_4N)_3[Nb_2Cl_9]$.

Shown in Figure 7 are plots of the measured molar susceptibilities versus temperature for $(Bu_4N)[Nb_2Cl_7(PEt_3)_2]$ (Figure 7a) and $(Et_4N)_2[Nb_2Cl_8(THT)]$ (Figure 7b), after diamagnetic corrections made by using Pascal's constants. It can be clearly seen that, except for the upward tail at very low temperature, the susceptibilities are very small and essentially temperature independent. The molar susceptibilities above 60 K are around 2.0×10^{-4} and 1.0×10^{-4} emu for the phosphine and the THT compounds, respectively. This temperature-independent paramagnetism is in agreement with the earlier observations on similar compounds by McCarley et al.[5] As the temperature goes below 40 K, the sharp increases of the susceptibilities can be attributed to unidentified paramagnetic impurities.

The temperature-independent paramagnetism (TIP) in $(Bu_4N)[Nb_2Cl_7(PEt_3)_2]$ and $(Et_4N)_2[Nb_2Cl_8(THT)]$ may be understood in terms of the calculated electronic structures of the model compounds. The manifestation of TIP in a molecular system characterized by a spin-singlet ground state is a typical second-order response property[20] and, as such, is sensitive to the spectrum of excited states. The TIP can be large if there exist accessible but not thermally populated low-lying excited states.[21] We have already seen that both $[Nb_2Cl_7(PH_3)_2]^-$ and $[Nb_2Cl_8SH_2]^{2-}$ (Figure 6) have a closed-shell singlet ground state and a set of low-lying excited states which can certainly be considered not accessible thermally even at room temperature. It is impossible from the current calculations to identify any specific state or states that may be important in making contributions to the observed TIP, but we may observe that the lowest singlet excited state $^1B_1$ is calculated to lie only 5000 and 7910 cm^{-1} above the ground state in the phosphine and the thioether compounds, respectively. Therefore, the occurrence of TIP would not be unexpected from the electronic structure calculations. The conclusion may also be drawn from the relatively simple $X\alpha$ molecular orbital calculations. Such calculations have predicted a closed-shell electronic configuration for the ground state and a set of low-lying virtual orbitals which then would imply low-lying excited states. There is also an interesting correlation between the measured TIP and the calculated energy differences. As can be seen in Figure 6, the energy differences between the ground state and the excited states in the phosphine compound are only about half of the differences in the thioether compound. Correspondingly, the observed TIP (2.0×10^{-4} emu/mol) in $(Bu_4N)[Nb_2Cl_7(PEt_3)_2]$ is twice as great as that (1.0×10^{-4} emu/mol) in $(Et_4N)_2[Nb_2Cl_8(THT)]$.

Experimental studies of the magnetic behavior of $(Et_4N)_3[Nb_2Cl_9]$ are currently in progress, as are efforts to relate the results to the calculated manifold of low-lying states shown in Figure 6. We shall reserve detailed discussion for a future report since the situation is very complex.

Acknowledgment. We thank the National Science Foundation for support. CRAY Research Inc. and the Department of Chemistry of Texas A&M University are thanked for granting computer time.

Supplementary Material Available: Complete tables of crystallographic data, full lists of bond distances and angles, tables of anisotropic thermal parameters, a table of positional parameters for the hydrogen atoms of $(Et_4N)_3(Nb_2Cl_9)\cdot 5CH_2Cl_2$, a table of least-squares planes for $(Pr_4N)_3[Nb_2Cl_9]\cdot 6CH_2Cl_2$, ORTEP packing diagrams, ORTEP views of the Et_4N^+ cations in $(Et_4N)_2[Ta_2Cl_8(THT)]$, and an ORTEP drawing of the $[Nb_2Cl_8(THT)]^{2-}$ ion (44 pages). Ordering information is given on any current masthead page.

(20) Buckingham, A. D. *Adv. Chem. Phys.* **1967**, *12*, 107.
(21) Van Vleck, J. H. *The Theory of Electric and Magnetic Susceptibilities*; Oxford University Press: London, 1932.